Electromagnetic lensing using a flat-glass Ferrocell

Timm A. Vanderelli

Principal Investigator at Ferrocell USA, Ligonier, PA. USA
Experimental Physics
Orchid ID: 0000-0002-2295-0272

Email address:
tvan@ferrocell.us (Timm Vanderelli)

Pre-print DRAFT November 2021

Abstract

In this report, I show by experiment how a *flat-glass* Ferrocell will create a circular disk pattern on a target using laser and an electromagnetic field from a Helmholtz coil in a similar manner as a glass Plano-concave lens does. Furthermore, I show how this circular pattern will increase or decrease in diameter, depending on the location of a Ferrocell between a laser source and target while induced within an electromagnetic field.

Keywords: Ferrocell, Ferrolens, Magneto-optics, Electromagnetism, Ferrofluid, Dynamic Thin-film, Helmholtz Coil, Light scattering, Laser, Nanotechnology, Magnetic lensing.

Introduction

A Ferrocell[1] or Ferrolens[2] is comprised of two flat disks of optical glass separated by a thin-film of Ferrofluid[3] and sealed around its circumference with an optical adhesive[4].
In recently published papers[5,6,7,8,9] written about the optical response of Ferrocells, other researchers have shown how this device will scatter light in a direction determined by the orientation of a magnetic field using externally applied permanent magnets and LED light sources. Here, I report how the cell responds when induced within the center of an electromagnetic field from an air-core Helmholtz coil[10] while irradiated by a low-power green laser[11]. For the following tests, two clear, 62mm diameter x 2 mm thick borosilicate flat glass disks were used, with a 30-micron layer of Ferrofluid equally dispersed and sealed between them. In this thin-film condition, the fluid layer is translucent instead of its normally opaque condition. During the following tests, the Ferrocell is operated in the transmission mode. Without an applied field, the fluid's suspended and coated magnetite nanoparticles exist in a Superparamagnetic state[12], functioning in a similar manner to a nonlinear, long-pass optical filter, exhibiting a high degree of absorption in the shorter wavelengths, as shown by spectrometer[19] in the following two Figures. A white Halogen light source was used as a reference *without* the cell installed as seen in Figure 1a. White light transmitted through and absorbed by a Ferrocell centrally located between both *un-activated* inductors of the Helmholtz coil is shown in Figure 1b.

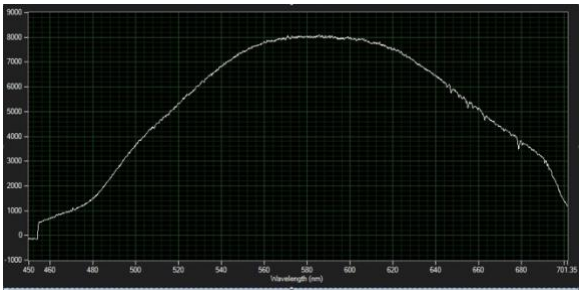

Figure 1a. Absorption spectrograph of white Halogen light for reference, without a Ferrocell. Y-axis indicates relative amplitude across visible spectrum.

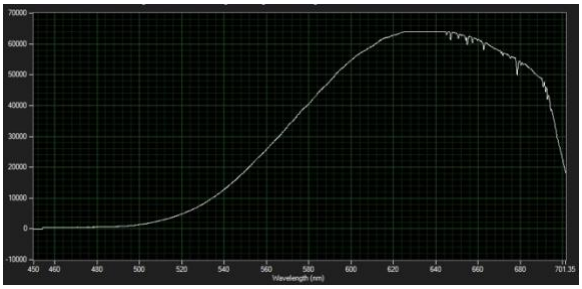

Figure 1b. Absorption spectrograph of white Halogen light transmitted through the 30 micron thin-film *without* an applied electromagnetic field. Y-axis indicates relative amplitude across visible spectrum.

However, with the application of an electromagnetic field, the nanoparticles form "chains[13]" that change the particles response into a ferrimagnetic state[14]. When in this state, the particle chains scatter light in a direction and a manner determined by the spatial orientation of the induced field[15]. The following tests and examples show how a Ferrocell, when located inside an air-core Helmholtz coil, will scatter laser into a circular beam pattern on a target, which is then compared to a circular pattern obtained from a glass, Plano-concave (PCV) glass lens[16], as shown in the following examples obtained through experiment.

Experiments

A simple test apparatus was fabricated using black ABS plastic through a 3-D printer and inserted into the center, between the two air-core Helmholtz inductors. A photo of this unit is shown in Figure 2 and Figure 3 shows a CAD drawing of it as an exploded view. This test apparatus consists of a laser source mounted into an insert located in the rear, south pole of the unit. An ABS plastic diaphragm with a one-millimeter diameter aperture was positioned 5 mm from the laser output. A first target consisting of a 55 mm circle of typical bright-white printer paper with a 2 mm black dot in the center and a thin grid of 10 mm squares was fixed into the opposing north pole insert at the front of this unit for taking photos without saturating the camera's CCD sensor by laser. A second target was constructed without a center dot or grid-lines using the same bright-white paper for use with the beam profiling camera[18], again to prevent saturation of its CCD sensor. The Ferrocell is positioned at a specific distance between electromagnetic poles within this light-proof tunnel, including any position inside of both front and rear inserts. In the following experiments, a Ferrocell was moved closer or farther away from the target while *inside the field* when irradiated with laser. These actions altered the outer diameter of the scattering pattern on the targets.

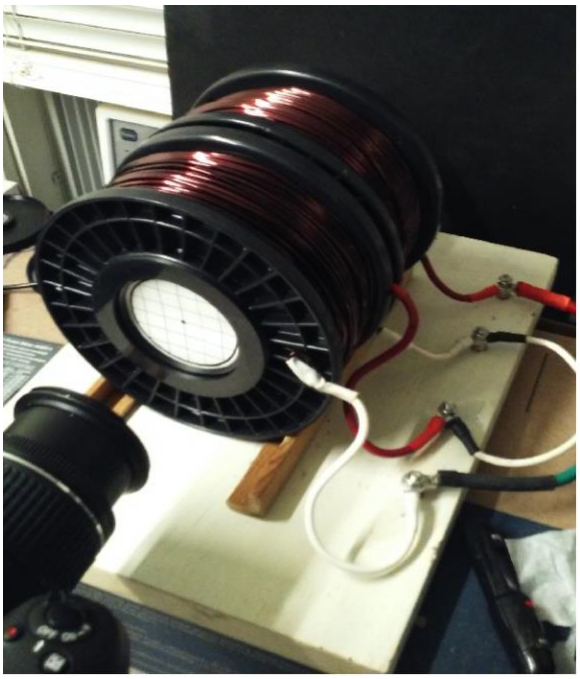

Figure 2. Photo of test apparatus inside Helmholtz coil. Target is located in the north polar edge of coil.

A series of tests were performed using this apparatus and their results were recorded using a digital camera, spectrometer, beam profiler camera and its associated software[20]. In a *first* experiment, a Ferrocell was centrally located inside the Helmholtz inductors, equidistant at 70 mm between laser aperture and target. Measured power output[21] from the laser's aperture was 10.5 mW (.0105 J/sec) at the source and was maintained within 1.1 percent throughout all the tests shown here. Measured power output from the Ferrocell was 850 µW, indicating 9.65 mW or .0097 J/sec of absorption in the Ferrofluid layer *without* an applied field. Input power to the Helmholtz coil was 600 Watts DC (20 VDC @ 30 A) for a duration of 10 seconds. Coil temperature was 22 C at the beginning of *each* test. A field strength of 914 Gauss was measured[22] in the center, between both inductors at this 70 mm location.

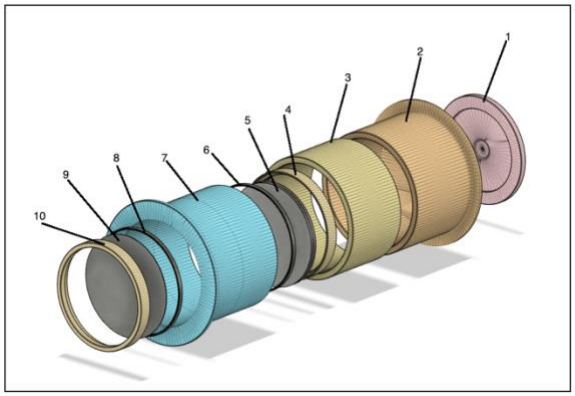

Figure 3. CAD drawing, exploded view of test apparatus inserted into Helmholtz coil.

[1] Aperture	[2] Rear insert	[3] Tunnel	[4] Lock ring A
[5] Ferrocell	[6] Lock ring B	[7] Front insert	[8] Lock ring C
	[9] Target	[10] Lock ring D	

Figure 3 legend

A digital camera photo of the first target and a reference laser beam *without* an induced field is shown in Figure 4a.

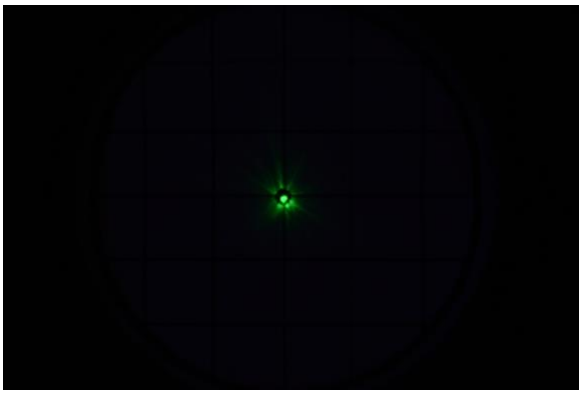

Figure 4a. Laser beam through Ferrocell, onto the center of the first target without an induced field.

A beam profile of the laser spot on the second target *without* an induced field is shown for a reference in Figure 4b.

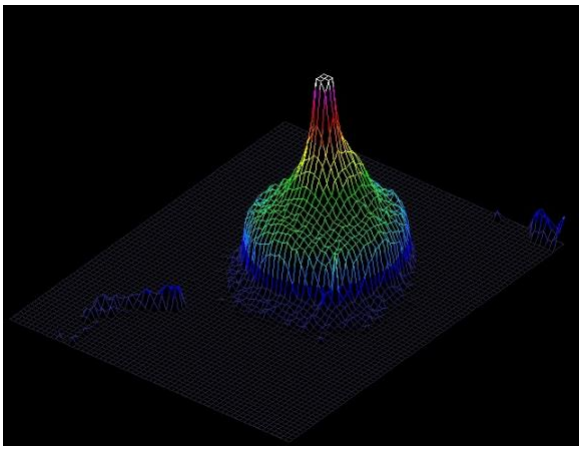

Figure 4b. Beam profile of laser beam spot through Ferrocell onto second target *without* an applied electromagnetic field. White tip is 2 mm in diameter.

During the ten second period after the coils were activated, a scattered circular pattern was resolved, filling the 55 mm target area and beyond its outer circumference, as shown in Figure 5a.

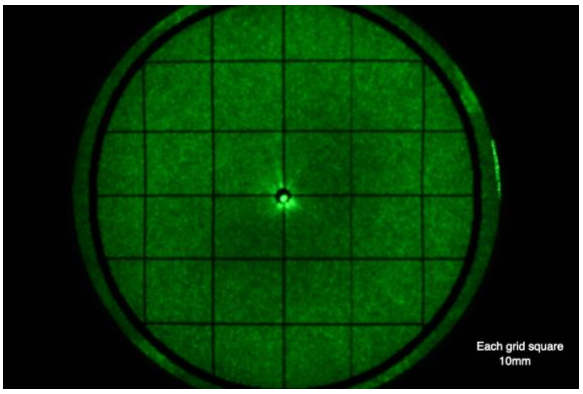

Figure5a. Field induced cell at 70 mm from target.

A spectrometer measurement of the beam amplitude, without using a target and expressed in relative units along the y-axis is shown in Figure 5b and a beam profile of the resulting scattering pattern, utilizing the second target, is shown in Figure 5c.

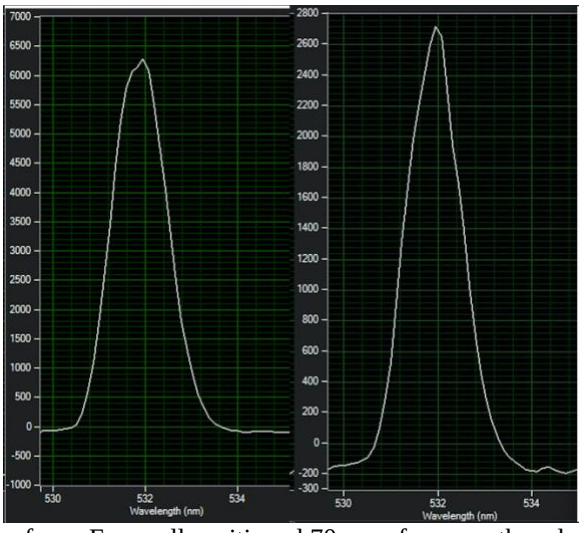

Figure 5b. Spectrometer graphs from Ferrocell positioned 70 mm from north edge. Y-axis relative amplitude reads 6250 without an induced field on left and 2750 with field, right.

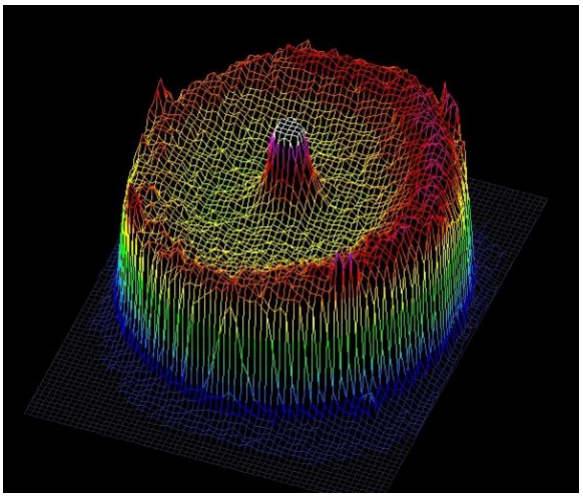

Figure 5c. Beam profile of second target with the cell positioned at a 70 mm distance with an induced field. Outer ring is 55 mm diameter and white peak is 5 mm.

One feature of this activity is worth mentioning. Immediately after dispersion of the laser begins, the center "spot" experiences a noticeable reduction of amplitude. During these tests, the change in amplitude was measured and compared both without and with an induced field, as indicated in the included spectrometer *Figures 5b, 6b and 7b* graphs. We see as the scattering progressed, the laser beam "spot" diminished approximately 60% in amplitude after 10 seconds of the applied electromagnetic field and this ratio increases slightly as the diameter of the circular beam decreases. In a *second* experiment, a Ferrocell was positioned closer to the target at a distance of 30 mm within a measured field strength of 885 Gauss. Figure 6a shows a photo of a resulting circular beam scattering pattern on the first target. The outside diameter of this ring measured 30 mm, compared to the previous experiment where the circular ring diameter was larger than the target's 55 mm outer circumference.

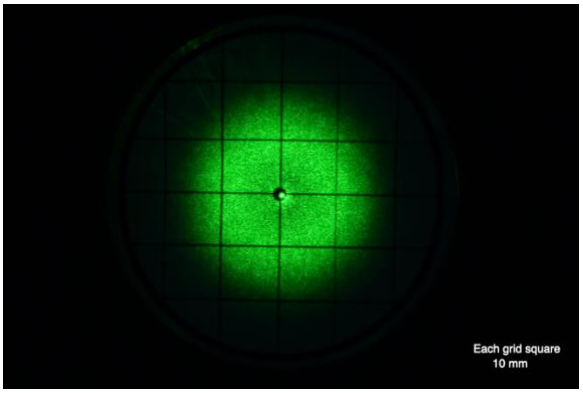

Figure 6a. Field induced cell at 30 mm from target.

Figure 6b shows the spectrometer results both with and without an induced field.

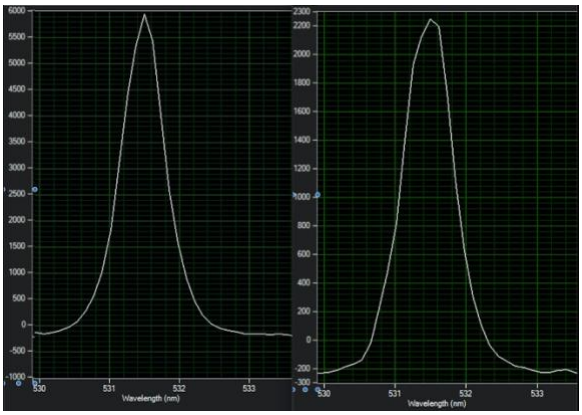

Figure 6b. Spectrometer graphs with Ferrocell positioned 30 mm from north edge. Y-axis relative amplitude is 6000 without an induced field on the left and 2250 with on the field on right.

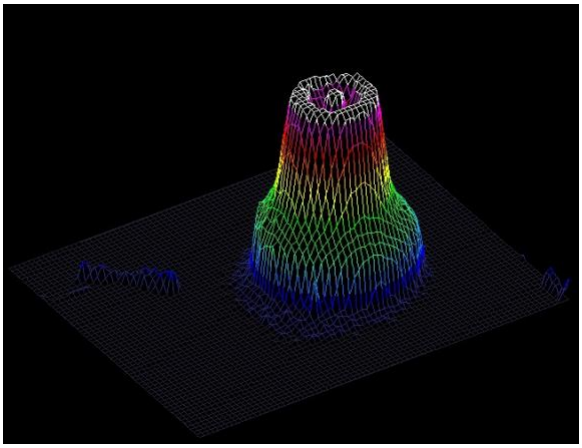

Figure 6c. Beam profile of second target with the cell positioned at a 30 mm distance with an induced field.

Figure 6c represents the resultant beam profile at a 30 mm distance from the second target as a 3-D graph. A *third* experiment was performed using a Ferrocell closer to the north polar end of the field into a measured strength of 837 Gauss. The cell was positioned to a distance of 20 mm from the target. Figure 7a shows a photo of the resulting circular pattern. The outside diameter of this ring was 20 mm, compared to the previous experiment where the ring was 30 mm outside diameter. Figure 7b shows the spectrometer results without a target and Figure 7c represents the beam profile as a 3-D graph, utilizing the second target.

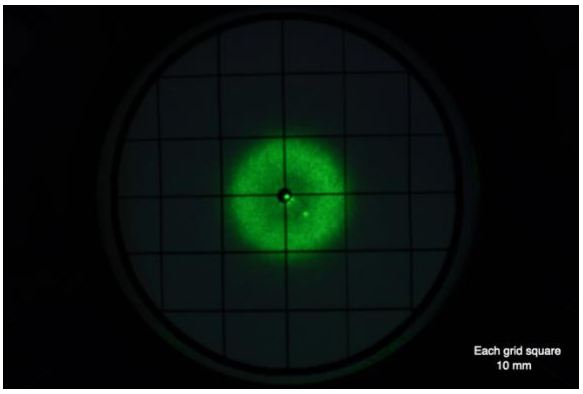

Figure 7a. Field induced cell at 20 mm from target.

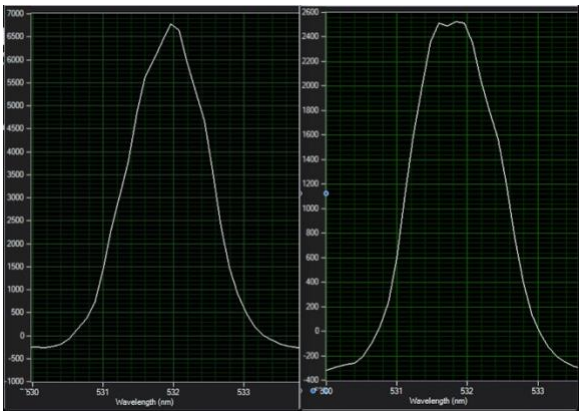

Figure 7b. Spectrometer graphs with Ferrocell positioned 20 mm from north edge. Y-axis relative amplitude is 6550 without field on left and 2500 with an induced electromagnetic field shown on right.

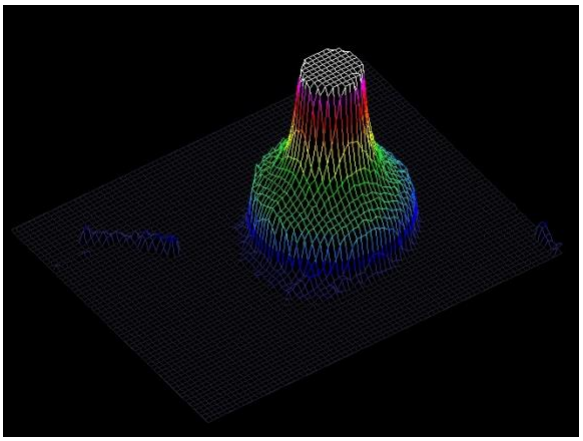

Figure 7c. Beam profile of second target with the cell positioned at a 20 mm distance with an induced field.

The *fourth* and final experiment for this report was performed for comparison between the electromagnetic lensing effect obtained from a flat-glass Ferrocell and a typical glass Plano-concave lens. A mounting plate for the concave lens was printed using black ABS plastic, and centrally positioned within the tunnel insert, *first* at an equal distance of 70 mm between aperture and target. The curved face of the concave lens was irradiated into its center by laser with

only 3 mW of output power to obtain a clear, unsaturated photo due to the negligible absorption from the glass. Figure 8a shows this recorded image.

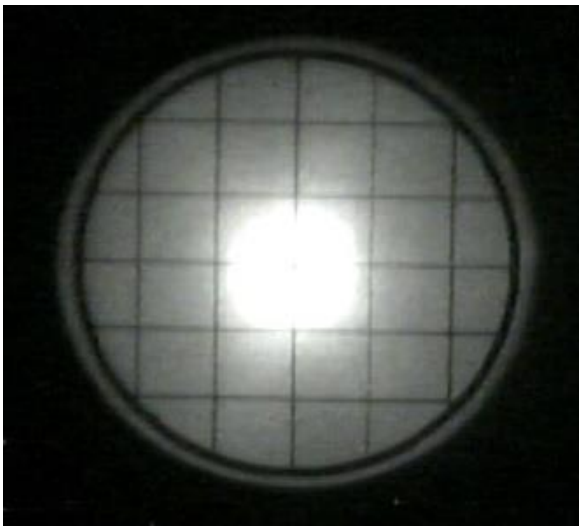

Figure 8a. Circular pattern image from Plano-concave lens, equidistant at 70 mm between aperture and first target using the beam profiling camera.

Figure 8b shows the 3-D profile of the glass Plano-concave lens's circular beam dispersion utilizing the first target at 70 mm.

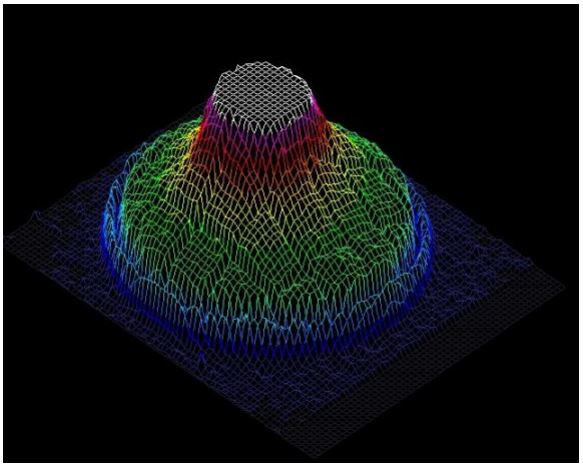

Figure 8b. Beam profile of the Plano-concave lens positioned at 70 mm distant from the first target.

And in a *second* test closer to the first target, Figure 8c shows a photo from the beam profiling camera of the Plano-concave lens irradiated with 3 mW laser output power at a distance of 35 mm away from the target.

Figure 8c. Circular pattern image of Plano-concave lens 35 mm from first target using beam profile camera.

Figure 8d shows a 3-D graphical representation of the Plano-concave lens beam profile at 35 mm distant from the first target. These two tests indicate the closer the lens is to the target, the smaller in diameter the resulting circular pattern becomes.

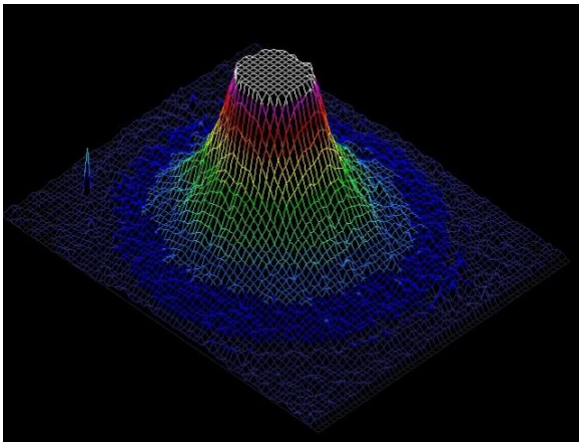

Figure 8d. Beam profile of the Plano-concave lens positioned at 35 mm distant from the first target.

Conclusion

I've shown by experiment how a flat-glass Ferrocell will respond when influenced by an electromagnetic field and irradiated with laser. And, how the curvature of the electromagnetic field is responsible for diffracting laser through the thin-film into a projected circular beam pattern. These tests indicate a lensing effect from an electromagnetically induced Ferrocell when positioned closer or farther away from the target, thereby altering the circular ring's outer diameter. Also, I've shown a strong correlation to this effect and the lensing effect of laser passing through a glass Plano-concave lens at alternate distances from the target. It should be noted that the *active region* of the Ferrocell, when illuminated by the laser is only a one-millimeter circular area and the high currents required to complete these experiments were necessary due to the large surface area of the Ferrocell. This apparatus could be made much smaller and more efficient, but those goals are not within the focus of this investigation. Obviously, I have not included any formulae or theories in this report, but only the data resulting from my experiments. More detailed

information about the Ferrocell is available from the published papers I've included here, and much more information can be obtained by searching for papers by other authors not mentioned in the references. Any of the experiments shown in this report can be easily duplicated by anyone with basic technical skills and I encourage experimental researchers with an interest in this topic to re-create these experiments to verify my findings and to publish their work. Please contact me with any questions on how to do so. I will make the 3-D printer files (stl's) available for the individual pieces of the featured apparatus and instructions on how to construct a Ferrocell, by request.

Acknowledgments

I would like to thank Dr. Alberto Tufaile and his wife, Dr. Adriana Pedrosa Biscaia Tufaile at the School of Arts, Sciences and Humanities in Sao Paulo, Brazil for their continuing support, research and collaboration over the past six years. Additionally, I would like to thank Michael M. Snyder from the University of Louisville, Kentucky, USA, Emmanouil Markoulakis at Hellenic Mediterranean University, Irakleion, Greece, Dr. Rasbindu V. Mehta and Vishakha Dave at Maharaja Krishnakumarsinhji Bhavnagar University, India for their continuing contributions and collaboration utilizing the Ferrocell.

References

[1] Ferrocell® is a registered US Trademark for the magneto-optic device generally known as a Ferrolens. https://www.ferrocell.us/intro.html Magnetic flux viewer. US patent 8246356, issued August 21, 2012 to the author.

[2] Ferrolens is the generic term for the US Trademarked Ferrocell®.

[3] Ferrotec USA. Product: EFH1 Ferrofluid. Saturation magnetization: 400 Gauss. Viscosity: 6 cp @ 27 C. Particle density: 1.21 gm/ml. https://www.ferrotec.com

[4] Norland #81, UV cured, optical adhesive. https://www.norlandprod.com/adhesives.html

[5] Alberto Tufaile, Timm A. Vanderelli, Adriana Pedrosa Biscaia Tufalie. "Light Polarization Using Ferrofluids and Magnetic Fields". January 2017, Advances in Condensed Matter Physics, 2017:1-7. DOI: 10.1155/2017/2583717

[6] Alberto Tufaile, Michael M. Snyder, Adriana Pedrosa Biscaia Tufalie. "Horocycles of Light in a Ferrocell". August 2021, Condensed Matter, 6(3):30. DOI:10.3390/condmat6030030

[7] Alberto Tufaile, Michael M. Snyder, Timm A. Vanderelli, Adriana Pedrosa Biscaia Tufalie. "Jumping Sundogs, Cat's Eye and Ferrofluids". July 2020 Condensed Matter, 5(3):45. DOI: 10.3390/condmat5030045

[8] Vishaka Dave, Rasbindu V. Mehta, SP Bhatnagar. "Extinction of light by a Ferrocell and ferrofluid layers: A comparison". May 2020 Optik, an International Journal for Light and Electron Optics

[9] Emmanouil Markoulakis, Timm Vanderelli, Lambros Frantzeskakis. "Real time display with the ferrolens of homogeneous magnetic fields". September 2021, Journal of Magnetism and Magnetic Materials, 541(1):168576. DOI: 10.1016/j.jmmm.2021.168576

[10] Helmholtz coil, consisting of two 140 mm outside diameter, 90 mm inside diameter, 45 mm wide spools. Each consisting of 68 meters of #12 square, enameled, copper wire and spaced apart 70 mm (center to center), with a combined (series connected) DC resistance of 400 milli-Ohms and a combined inductance of 4 mH.

[11] Laser, one-Watt, 532 nm with a zero to full output, precision, variable power supply.

[12] R. V. Mehta. "Polarization dependent extinction coefficients of superparamagnetic colloids in transverse and longitudinal configurations of magnetic field". February 2014. Elsevier - Optical Materials. 1436-1442

[13, 14] Alexey O. Ivanov, Andrey Zubarev. "Chain formation and Phase Separation in Ferrofluids: The Influence on Viscous Properties". September 2020; 13(18): 3956 MDPI (Materials). DOI: 10.3390/ma13183956

[15] R. E. Rosensweig, "Ferrohydrodynamics". Dover publishing 1997. Pages 178-179

[16] Lens, Plano-concave, 35 mm diameter x 6 mm thick, VIS coated, frosted, BK-7 glass.

[17] Digital camera, Nikon D7200 with AF-P Nikkor 18-55 mm lens, manual focus. Manual camera settings: F11, ISO 125. No flash.

[18] Beam profiling digital camera, NEC 38-0620 monochrome CCD with 8 mm, F-1.3 zoom lens, manual focus.

.

[19] Spectrometer, Czerny-Turner design with 1800 lines/mm reflection grating. Sony ILX511 linear CCD sensor. Spectrum Studio 1.3 graphical interface software.

[20] Beam profiling software, Beamview 4.8.1

[21] Laser power meter, SPER Scientific 840011.

[22] Gaussmeter, Alpha Labs GM-2.